Video Article

Effect of Bending on the Electrical Characteristics of Flexible Organic Single Crystal-based Field-effect Transistors

Man-Tzu Ho[1,2], Yu-Tai Tao[1]

[1]Institution of Chemistry, Academia Sinica

[2]Department of Chemistry, National Central University

Correspondence to: Yu-Tai Tao at ytt@gate.sinica.edu.tw

URL: https://www.jove.com/video/54651
DOI: doi:10.3791/54651

Keywords: Engineering, Issue 117, flexible electronics, field-effect transistor, single crystal device, bended crystal, crystal packing, charge mobility

Date Published: 11/7/2016

Citation: Ho, M.T., Tao, Y.T. Effect of Bending on the Electrical Characteristics of Flexible Organic Single Crystal-based Field-effect Transistors. *J. Vis. Exp.* (117), e54651, doi:10.3791/54651 (2016).

Abstract

The charge transport in an organic semiconductor depends highly on the molecular packing in the crystal, which influences the electronic coupling immensely. However, in soft electronics, in which organic semiconductors play a critical role, the devices will be bent or folded repeatedly. The effect of bending on the crystal packing and thus the charge transport is crucial to the performance of the device. In this manuscript, we describe the protocol to bend a single crystal of 5,7,12,16-tetrachloro-6,13-diazapentacene (TCDAP) in the field-effect transistor configuration and to obtain reproducible I-V characteristics upon bending the crystal. The results show that bending a field-effect transistor prepared on a flexible substrate results in nearly reversible yet opposite trends in charge mobility, depending on the bending direction. The mobility increases when the device is bent toward the top gate/dielectric layer (upward, compressive state) and decreases when bent toward the crystal/substrate side (downward, tensile state). The effect of bending curvature was also observed, with greater mobility change resulting from higher bending curvature. It is suggested that the intermolecular π-π distance changes upon bending, thereby influencing the electronic coupling and the subsequent carrier transport ability.

Video Link

The video component of this article can be found at https://www.jove.com/video/54651/

Introduction

Soft electronic devices, such as sensors, displays, and wearable electronics, are currently being designed and researched more actively, and many have even been launched in the market in recent years[1,2,3,4]. Organic semiconducting materials play an important role in these electronic devices due to their inherent advantages, including low development cost, the ability to be prepared in solution or at low temperatures, and, in particular, their flexibility when compared to inorganic semiconductors[5,6]. One special consideration for these electronics is that they will be subjected to frequent bending. Bending introduces strain in the components and the materials within the device. A stable and consistent performance is required as such devices are bent. Transistors are a vital component in most of these electronics, and their performance under bending is of interest. A number of studies have addressed this performance issue by bending organic thin film transistors[7,8]. While the changes in conductance upon bending may be attributed to the changes in spacing between the grains in a polycrystalline thin film, a more fundamental question to ask is whether the conductance may change within a single crystal upon bending. It is well accepted that charge transport between organic molecules depends strongly on electronic coupling between molecules and the reorganization energy involved in the interconversion between the neutral and charged states[9]. Electronic coupling is highly sensitive to the distance between neighboring molecules and to the overlap of frontier molecular orbitals. The bending of a well-ordered crystal introduces strain and may change the relative position of molecules within the crystal. This can be tested with a single crystal-based field-effect transistor. One report used single crystals of rubrene on a flexible substrate to study the effect of crystal thickness upon bending[10]. Devices with copper phthalocyanine nanowire crystals prepared on a flat substrate were shown to have a higher mobility upon bending[11]. However, the properties for an FET device bent in different directions have not been explored.

The molecule 5,7,12,16-tetrachloro-6,13-diazapentacene (TCDAP) is an n-type semiconductor material[12]. The crystal of TCDAP has a monoclinic packing motif with shifted π-π stacking between neighboring molecules along the *a* axis of the unit cell at a cell length of 3.911 Å. The crystal grows along this packing direction to give long needles. The maximum n-type field-effect mobility measured along this direction reached 3.39 $cm^2/V \cdot sec$. Unlike many organic crystals that are brittle and fragile, TCDAP crystal is found to be highly flexible. In this work, we used TCDAP as the conducting channel and prepared the single crystal field-effect transistor on a flexible substrate of polyethylene terephthalate (PET). Mobility was measured for the crystal on a flat substrate, with the device bent toward the flexible substrate (downward) or bent toward the gate/dielectric side (upward). *I-V* data were analyzed based on changes in the stacking/coupling distance among the neighboring molecules.

Protocol

1. Preparation of TCDAP[12]

1. Synthesize TCDAP by following literature procedures[13].
2. Purify the TCDAP product by the temperature-gradient sublimation method, with the three temperature zones set at 340, 270, and 250 °C, respectively, under a vacuum pressure of 10^{-6} Torr[12,14].

2. Grow Single Crystals of TCDAP Using a Physical Vapor Transfer (PVT) System[14]

1. Put the TCDAP sample at one end of a boat (5 cm long) and load the boat into a glass inner tube (15 cm long with a diameter of 1.2 cm).
2. Load the inner tube into a longer glass tube (83 cm long and 2 cm in diameter) and push it in to about 17 cm from the opening.
3. Load the long glass tube into a copper tube (60 cm long and 2.5 cm in diameter) horizontally fixed on a rack; make sure the boat of TCDAP is located in the middle of the heating area defined by a heating band around the copper tube.
4. Purge the PVT system with helium gas at a flow rate of 30 cc/min, and then turn on the transformer to heat up the heating band to 310 °C; maintain at this temperature for two days.
5. After cooling the system to room temperature, collect the crystals from the inner tube.

3. Device Fabrication

1. Put a 200-μm-thick, transparent, pre-cut PET substrate (2 cm x 1 cm) into a vial and clean it by sonication in detergent solution, deionized water, and acetone, in sequence, for 30 min each. Dry the substrate by nitrogen flow.
2. Place double-sided tape on the PET substrate.
3. Examine the crystals under a stereomicroscope. Select good quality, shining crystals with a dimension of ~5 mm x ~0.03 mm for device fabrication. Place a needle-like TCDAP crystal parallel with the length of the PET substrate on the double-sided tape and fix it securely.
4. Under a stereomicroscope, apply water-based colloidal graphite through a microliter syringe needle in a line (several mm) that extends from the two ends of the crystal acting as the source and drain. Wait for about 30 min for the colloidal graphite to dry and measure the distance between the two graphite spots under an optical microscope to determine the exact channel length (keep it at 0.6-1 mm).
5. Use carbon conductive tape to fix the PET substrate on a microscopic slide. Place the slide near the end of the pyrolysis tube of the deposition chamber.
6. Weigh 0.5 g of the precursor of the dielectric insulator, [2.2]paracyclophane, and place it near the inlet of the pyrolysis tube.
7. Pump down the system to a vacuum of 10^{-2} Torr. Pre-heat the pyrolysis zone near the center of the tube up to a pre-set temperature of 700 °C and maintain at this temperature.
8. Heat up the [2.2]paracyclophane sample to 150 °C. The vapors of the precursor will pass through the pyrolysis zone to give the monomers, which will condense near the end of the pyrolysis tube to polymerize.
9. Let the pyrolysis/polymerization reaction continue for 2 hr.
10. Cool down the system and take out the samples from the pyrolysis tube.
11. Determine the thickness of the deposited dielectric layer by measuring the step height of the layer and substrate using a profilometer according to the manufacturer's instructions.
12. Apply isopropanol-based colloidal graphite through a microliter syringe needle in a line on the back of the dielectric layer above the crystal to serve as the gate electrode.

4. Measure the Performance of the Device

1. Use the scalpel to cut a hole through the polymeric dielectric film above the source/drain electrode area in order to expose the electrodes underneath for connection.
2. With the help of a stand and clamps, bring the electrode probes from the Parameter Analyzer into contact with the source/drain/gate electrodes. Record the I-V characteristics at different gate potentials according to the manufacturer's instructions.
   Note: Here, the gate potentials are set from -60 V to 60 V at 15 V steps.

5. Bending Experiments

1. To measure the properties in the tensile state, wrap the backside of the flexible PET substrate around cylinders of different radii (14.0 mm, 12.4 mm, 8.0 mm, and 5.8 mm) and fix the PET substrate to the cylinder on four sides with vacuum tape.
2. Connect the probes to the source/drain/gate electrodes and measure the I-V characteristics at different gate potentials as described in 4.2.
3. To measure in the compressive state, wrap half of the front side of the PET substrate around the end of a cylinder, such that the crystal/source/drain/gate electrodes are facing the cylinder and yet are still exposed. Fix the PET substrate on the cylinder with vacuum tape (see **Fig. 5**).
4. Connect the probes to the source/drain/gate electrodes and measure the I-V characteristics at different gate potentials as described in 4.2.
   NOTE: A cross-sectional illustration of the device structure is shown in **Fig. 1**.

Representative Results

The single crystal XRD analysis reveals that TCDAP is an extended π system with molecules packing along the *a* axis. **Fig. 2** shows the scan pattern by powder XRD for a TCDAP crystal. A series of sharp peaks are observed, corresponding only to the family of (0,k,ℓ) planes, by comparing with the powder diffraction pattern of the crystal. This would imply that the crystal structure is oriented as shown in **Fig. 3**.

Before bending, the flat n-type TCDAP single-crystal transistor gave well-resolved saturation currents only for positive gate voltages (V_{GS}) when the gate voltage was varied from -60 V to 60 V in 15 V steps. This suggests n-type behavior (**Fig. 4a**). **Fig. 4b** shows both the log (blue line) and the linear (black line) plots of the drain current as a function source-drain bias (V_{DS}) at a gate bias of 30 V.

The electron mobility was calculated from the I-V characteristics in the linear regime according to the equation,

$$I_D = \mu C_i \frac{W}{L}\left((V_{GS} - V_{TH})V_{DS} - \frac{V_{DS}^2}{2}\right) \quad (1)$$

or in the saturation regime according to the equation,

$$I_D = \mu C_i \frac{W}{2L}(V_{GS} - V_{TH})^2 \quad (2)$$

where W is the channel width, L is the channel length, m is the carrier mobility, C_i is the capacitance per unit area of the dielectric insulator, and V_{TH} is the threshold voltage, respectively.

An average mobility of 1.42 $cm^2/V{\cdot}sec$ and an on/off ratio of 10^3-10^4 were achieved.

For the bending experiment, bending of the ends downward should induce a stretch of the conduction channel near the channel/dielectric interface so that this is defined as the "tensile" state (see **Fig. 5a**), whereas bending of the ends upward will induce a compression of the conducting channel and is thus defined as the "compressive" state (see **Fig. 5b**). The *I-V* characteristics of the device in its flat state were checked after opposite bending operations to the curved state, with a radius R = 14.0 mm; the off-current virtually did not change (see **Fig. 6**). This served to indicate that the device structure is restorable and that the device was not destroyed upon bending in different directions. Next, the I-V was measured at the bent state for the tensile state. As shown in **Fig. 7a**, the current decreased with bending, more so with more bending (smaller radius). The calculated mobility was plotted as a function of the radius of bending. As shown in **Fig. 8a**, there is a clear trend of decreased mobility with increased bending. Thus, a downward bend at R = 14.0 mm caused a reduction of the mobility by 6.25%. Mobility reductions by 12.5%, 25%, and 37.5% for bending radii at 12.4 mm, 8.0 mm, and 5.8 mm, respectively, were observed. In contrast, when the device was bent upward (compressive state) at R = 14.0 mm, a slight shift in the linear I-V curve was observed, with an increased shift as bending increased (**Fig. 7b**). The calculated mobility based on the slope of the curves increased by 5.5%, 12.8%, 15.2%, and 19.8% for bent radii of 14.0 mm 12.4 mm, 8.0 mm, and 5.8 mm, respectively (**Fig. 8b**).

In a bent crystal, different sides experience different strains. On the concave side, the molecules are compressed, and on the convex side, the molecules spread apart, to an extent depending on the curvature. Thus, the upward and downward bending of crystal result in compression and spread of the molecules, respectively, at the gate dielectric interface, giving an increasing and decreasing electronic coupling, respectively.

The charge carriers in a transistor are known to be within several monolayers of the dielectric surface, and the mobility is mainly affected by the immediate layers next to the dielectric layer. In the current case, the increasing mobility in the compressive state and decreasing mobility in the tensile state should most likely be due to the change in intermolecular spacing within the crystal. Our results further testify to the importance of electronic coupling as a function of intermolecular distance. In a thin film device with polycrystalline grains, where the crystals may not be as big as we used in these experiments, the distance between grains can also be affected by bending, thereby generating similar results.

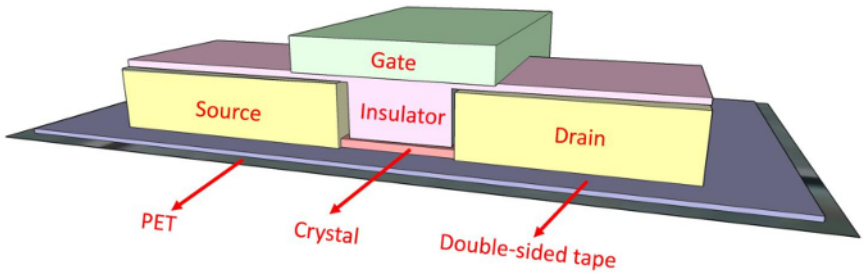

Figure 1. Cross-sectional illustration of the top-contact single crystal field-effect transistor prepared on a flexible substrate. The source/drain/gate electrodes were prepared from colloidal graphite, whereas the dielectric insulator was prepared from pyrolysis of the [2.2]paracyclophane precursor. Please click here to view a larger version of this figure.

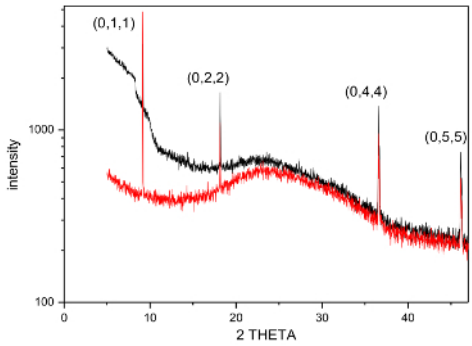

Figure 2. Powder X-ray diffraction pattern of the TCDAP single crystal laid on the PET substrate. The peaks were indexed to the family of (0,k,ℓ) planes. Please click here to view a larger version of this figure.

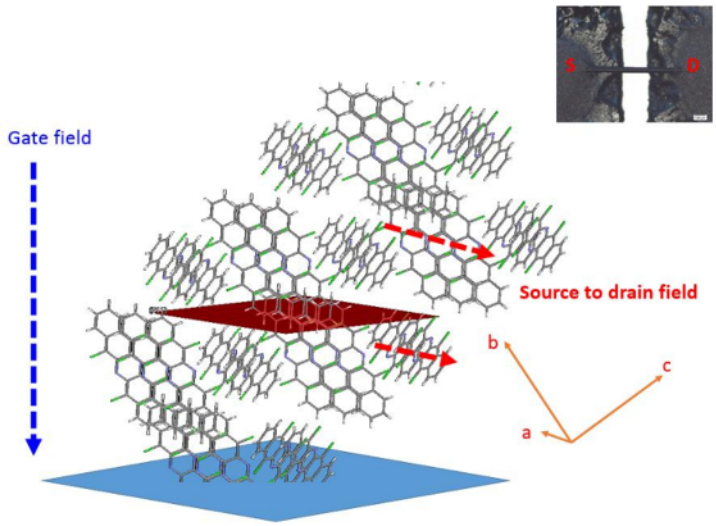

Figure 3. Schematic illustrations of the charge transport pathway. The charge transport along the *a* axis, with the (0,1,1) plane (red plane) parallel to the substrate (blue plane). Please click here to view a larger version of this figure.

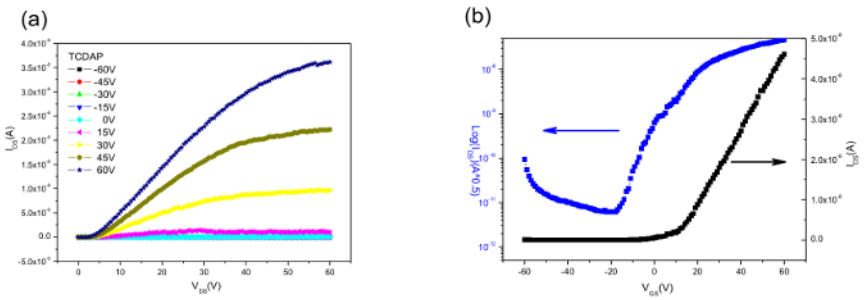

Figure 4. I_{DS}-V_{DS} characteristics. (**a**) The output characteristics with the gate voltage varied from -60 V to 60 V in 15 V steps and (**b**) the transfer characteristics, which show both the log (blue line) and linear (black line) plots of the drain current as a function of source-drain bias (V_{DS}) at a gate bias of 30 V for a TCDAP single crystal field-effect transistor (SCFET) on a PET substrate before bending. Please click here to view a larger version of this figure.

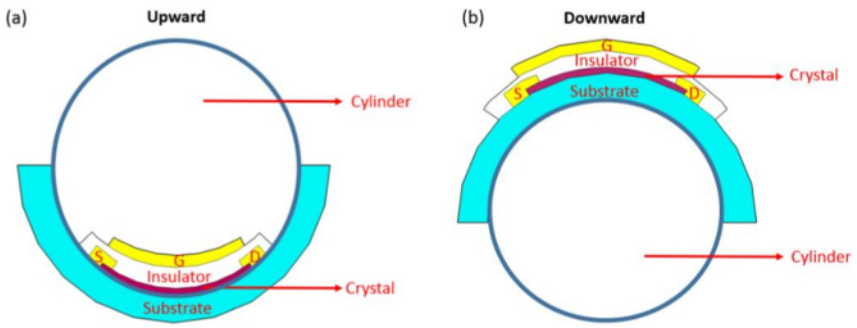

Figure 5. Schematic illustrations of the bending experiments. (**a**) The upward bending state, with the edge of the substrate wrapped around a cylinder while the device part is exposed, and (**b**) the downward bending state, with the substrate wrapped around a cylinder. Please click here to view a larger version of this figure.

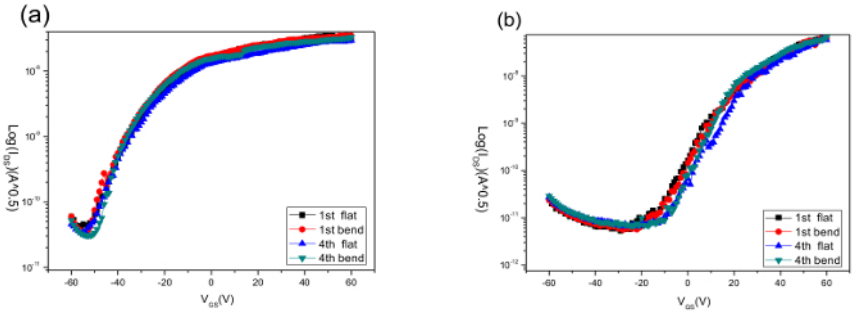

Figure 6. Comparison of transfer characteristics of the TCDAP single crystal-based FET device. Before and after (**a**) downward bending and (**b**) upward bending the first time and the fourth time to a curvature R = 14.0 mm. Please click here to view a larger version of this figure.

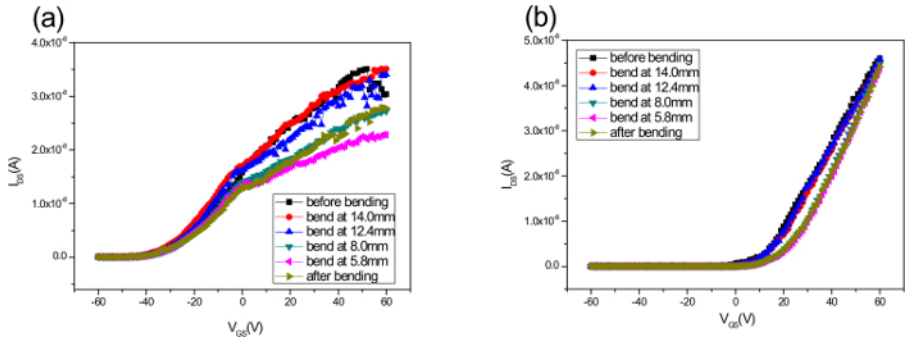

Figure 7. An overlay of the transfer characteristics of the TCDAP single crystal-based FET device. Bent state for (**a**) downward bending, and (**b**) upward bending in different bending radii (R = 14.0 mm, R = 12.4 mm, R = 8.0 mm, and R = 5.8 mm). Please click here to view a larger version of this figure.

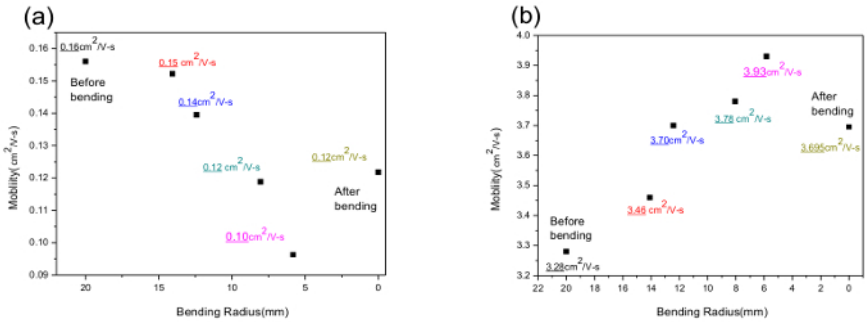

Figure 8. Measured mobility as a function of the bending radius for the TCDAP single crystal-based device. (**a**) Downward bending. (**b**) Upward bending. Please click here to view a larger version of this figure.

Discussion

In this experiment, a number of parameters affect the successful measurement of the field-effect mobility. Firstly, the single crystal should be large enough to be fabricated into a field-effect device for property measurement. The physical vapor transfer (PVT) method is the one that allows larger crystals to be grown. By adjusting the temperature and the flow rate of the carrier gas, crystals of sizes up to half a centimeter can be obtained. Secondly, the choice of a single crystal is important. An apparent single crystal may contain bundles of crystals, and bending may cause dissembling of the bundles. Thus, a thinner crystal is preferred. Thirdly, doubled-sided tape is necessary to keep the crystal in constant contact with the substrate surface, as extensive experiments showed that without such tape, the contacts between the crystal and the dielectric layer and/or electrode may shift upon multiple bending operations, so that the contact resistance increases and unstable or irreproducible current measurements are obtained. Another issue is in achieving the compressive state, when the ends of crystal are bent upward. When wrapping the flexible substrate around a cylinder of the proper diameter, the crystal/source/drain/gate have to be accessible by the probes. This is done by wrapping the edge of the flexible PET substrate around the end of the cylinder, so that the source/drain/gate area are exposed and accessible to the probes while maintaining the curved substrate.

In terms of data analysis, it is acknowledged that bending of the flexible substrate might cause a change in the thickness of the dielectric layer and in the capacitance. Although this possible change is not considered in the calculation of the mobility, it is noted that this change should be independent of the direction of the bending. However, the opposite trend in mobility changes should eliminate the possibility of mobility changes being due to the capacitance change. The quality of a single crystal will have much influence on the measured mobility. For the data shown in **Figure 8**, a wide difference in mobility was observed for the two crystals, presumably due to the quality of the crystals chosen. Nevertheless, the trends of the mobility change upon bending, which is of major concern in this work, form the basis for the conclusions derived from the experiments.

In contrast to current technology[11], where a crystal is first bent and then placed on a flat substrate for measurement, our method allows the measurement of current in the tensile state as well as the compressive state. In the previous technique, only the current passing through the shortest path, that is, the compressive state, can be measured. This method allows a variety of electrical properties to be measured directly on flexible substrates.

Disclosures

The authors have nothing to disclose.

Acknowledgements

This work was supported by the Ministry of Science and Technology, Taiwan, Republic of China through Grant No. 101-2113-M-001-006-MY3.

References

1. Sekitani, T., Zschieschang, U., Klauk, H., Someya, T. Flexible Organic Transistors and Circuits with Extreme Bending Stability. *Nat. Mater.* **9**, 1015-1022 (2010).
2. Yang, Y., Ruan, G., Xiang, C., Wang, G., Tour, J. M. Flexible Three-Dimensional Nanoporous Metal-Based Energy Devices. *J. Am. Chem. Soc.* **136**, 6187-6190, (2014).
3. Zhan, Y., Mei, Y., Zheng, L. Materials Capability and Device Performance in Flexible Electronics for the Internet of Things. *J. Mater. Chem. C.*, **2**, 1220-1232, (2014).
4. Zhang, L., Wang, H., Zhao, Y., Guo, Y., Hu, W., Yu, G.; Liu, Y. Substrate-Free Ultra-Flexible Organic Field-Effect Transistors and Five-Stage Ring Oscillators. *Adv. Mater.*, **25**, 5455-5460 (2013).
5. Jedaa, A., Halik, M. Toward Strain Resistant Flexible Organic Thin Film Transistors. *Appl. Phys. Lett.* **95**, (2009).
6. Nomura, K., Ohta, H., Takagi, A., Kamiya, T., Hirano, M., Hosono, H. Room-Temperature Fabrication of Transparent Flexible Thin-Film Transistors Using Amorphous Oxide Semiconductors. *Nature.* **432**, 488-492, (2004).
7. Sekitani, T. *et al.* Bending Experiment on Pentacene Field-Effect Transistors on Plastic Films. *Appl. Phys. Lett.* **86**, 073511, (2005).
8. Tseng, C.-W., Huang, D.-C., Tao, Y.-T. Organic Transistor Memory with a Charge Storage Molecular Double-Floating-Gate Monolayer. *ACS Appl. Mater. Interfaces.* **7**, 9767-9775, (2015).
9. Coropceanu, V., Cornil, J., da Silva Filjo, D. A., Olivier, Y., Silbey, R., Bredas, J. L. Charge Transport in Organic Semiconductors. *Chem. Rev.* **107**, 926-952, (2007).
10. Briseno, A. L. *et al.* High-Performance Organic Single-Crystal Transistors on Flexible Substrates. *Adv. Mater.* **18**, 2320-2324 (2006).
11. Tang, Q. *et al.* Organic Nanowire Crystals Combing Excellent Device Performance and Mechanical Flexibility. *Small.* **7**, 189-193 (2011).
12. Islam, M. M., Pola, S., Tao, Y.-T. High Mobility N-Channel Single-Crystal Field-Effect Transistors Based on 5,7,12,14-Tetrachloro-6,13-Diazapentacene. *Chem. Commun.* **47**, 6356-6358, (2011).
13. Weng, S. Z. *et al.* Diazapentacene Derivatives as Thin-Film Transistor Materials: Morphology Control in Realizing High-Field-Effect Mobility. *ACS Appl. Mater. Interfaces.* **1**, 2071-2079, (2009).
14. Kloc, C., Simpkins, P. G., Siegrist, T., Laudise, R. A. Physical Vapor Growth of Centimeter-Sized Crystals of A-Hexathiophene. *J. Cryst. Growth.* **182**, 416-427, (1997).

